Selective Stabilization of Natively Folded RNA Structure by DNA Constraints

Joseph P. Gerdt, Chandrasekhar V. Miduturu and Scott K. Silverman*

Department of Chemistry, University of Illinois at Urbana-Champaign, 600 South Mathews Avenue, Urbana, Illinois 61801

Oligonucleotides

Oligonucleotides were prepared and purified as described previously.[1] The complementary 14 bp constraint strands were 5′-TCGCCGTCCACCCA-3′ (attached at U144 or U142) and 5′-TGGGTGGACGGCGA-3′ (attached at U244 or U243). The complementary 12 bp constraint strands were 5′-TCGCCGTCCACA-3′ (attached at U144 or U142) and 5′-TGTGGACGGCGA-3′ (attached at U244 or U243).

Synthesis of RNA-DNA conjugates

RNA-DNA conjugates were prepared from four RNA segments as shown in Figure S1, using the general procedures described previously.[1,2]

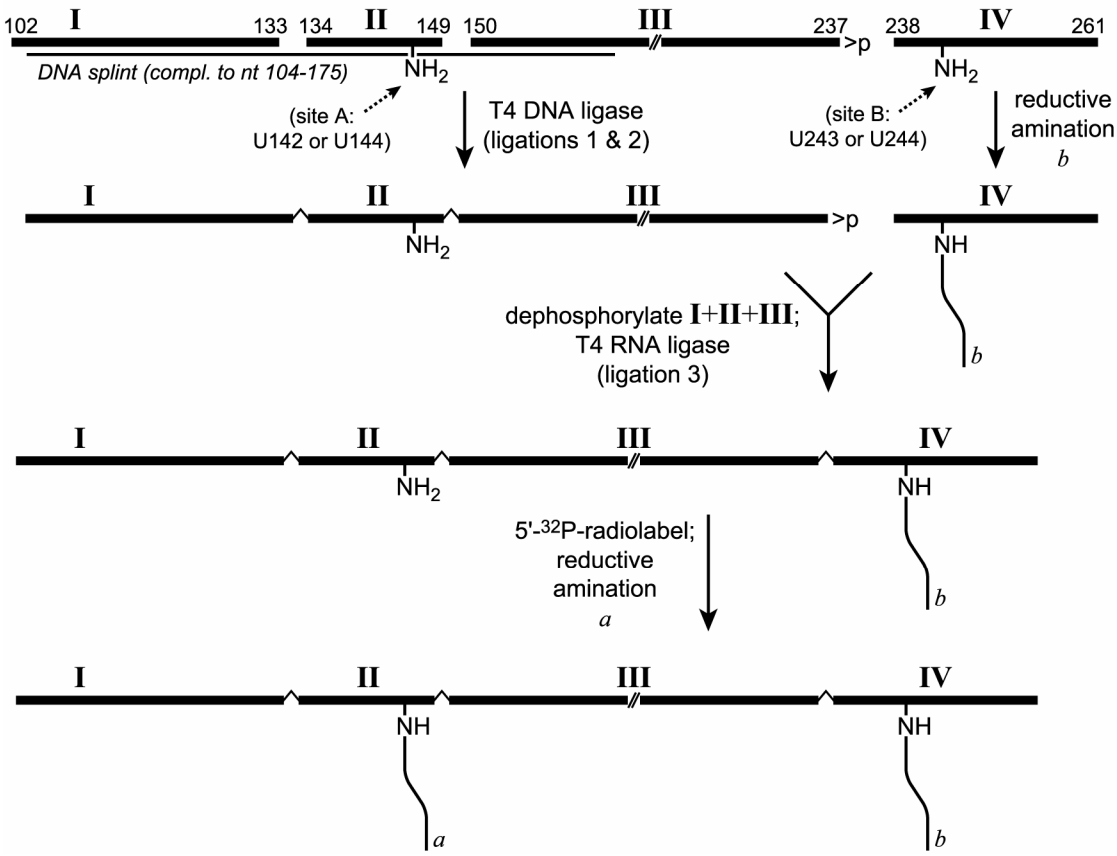

Figure S1. Strategy for synthesis of RNA-DNA conjugates.

Computer modeling

DNA duplexes of length 10–20 bp (in 2 bp increments) were placed manually near the desired P4-P6 attachment sites and covalently attached to the RNA 2′-positions. The remainder of the computer modeling was performed as described previously.[1] The minimized structures were evaluated visually with regard to disruption of the DNA duplex. For the U144/U244 and U142/U243 attachment sites on P4-P6, both the 14 bp and 12 bp DNA constraints appeared compatible with the natively folded RNA conformation (e.g., Figure 2B).

Nondenaturing polyacrylamide gel electrophoresis (native PAGE) experiments and data fitting

The native PAGE experiments were performed as described previously.[1] The relative gel mobility data for wild-type (wt) P4-P6 were fit to the titration equation[3] $M_{obs} = (M_{low} + M_{high} \bullet K \bullet [Mg^{2+}]^n)/(1 + K \bullet [Mg^{2+}]^n)$, where M_{obs} is the observed relative mobility F/N as a function of $[Mg^{2+}]$; M_{low} and M_{high} are the limiting low and high values of relative mobility; and K and n are the equilibrium constant and Mg^{2+} Hill coefficient for the simple model equation $U + nMg^{2+} \leftrightarrows F \bullet nMg^{2+}$ (U = unfolded state, F = folded state). The Mg^{2+} midpoint ($[Mg^{2+}]_{1/2}$ value) is $K^{-1/n}$. However, this titration equation could not satisfactorily fit the observed relative mobilities for the DNA-constrained P4-P6 RNAs because of the downward trend observed at high $[Mg^{2+}]$ (see data sets for DNA-constrained RNAs in Figure 3). Our explanation for this behavior is straightforward; a schematic model is shown in Figure S2. Although the foldable versions of the constrained RNAs maintain a maximum mobility plateau at $[Mg^{2+}] > 1$ mM, the J5/5a base-paired[4] (bp, nonfoldable) version of each DNA-constrained RNA becomes more mobile with increasing $[Mg^{2+}]$, because the unduplexed DNA strands can adopt a more compact conformation. This phenomenon was not observed in our previous studies where the DNA constraints destabilize RNA folding.[1,5] In those efforts, the DNA duplex was compatible with the nonfoldable variant throughout the range of $[Mg^{2+}]$, and therefore no unduplexed DNA strands were available for compaction at higher $[Mg^{2+}]$.

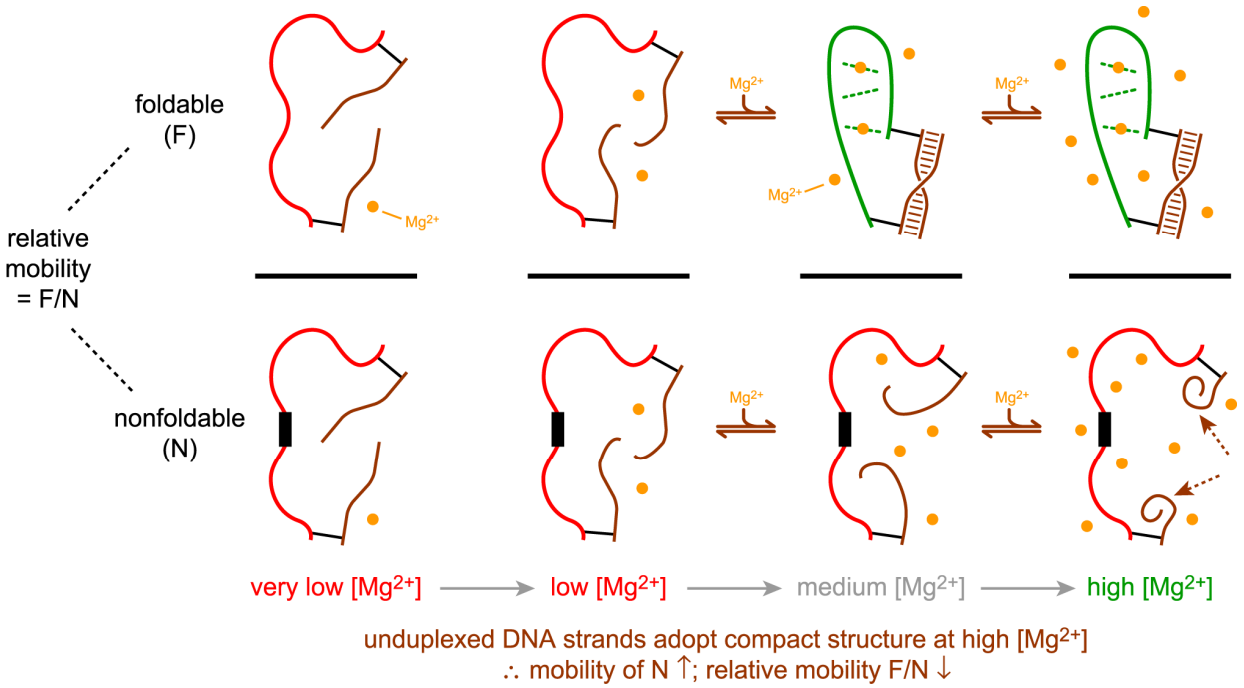

Figure S2. Model to explain the origin of the downward trend in observed relative mobility at high $[Mg^{2+}]$ when P4-P6 has an attached DNA constraint that is incompatible with the unfolded state. This downward trend at high $[Mg^{2+}]$ is observed (Figure 3B) when the reference RNA used for computing relative mobilities is nonfoldable with attached DNA constraints, as illustrated here. However, as explained on the bottom of page S3, this trend is instead observed at very *low* $[Mg^{2+}]$ (Figure S4) when the reference RNA used for computing relative mobilities is nonfoldable *without* attached DNA constraints.

This phenomenon is quantified in Figure S3, where the experimental mobility of each DNA-constrained P4-P6-bp variant relative to unconstrained P4-P6-bp is plotted against $[Mg^{2+}]$. The relative mobilities for each constrained RNA are calculated as F/N (i.e., relative mobilities of the foldable and nonfoldable versions), and the nonfoldable mobility is in the denominator of F/N. Therefore, the increasing mobility of the nonfoldable DNA-constrained RNAs leads to a decrease in relative mobility at high $[Mg^{2+}]$ specifically for these RNAs, but not for the unconstrained P4-P6.

The relative mobility titration equation was readily modified to account for this phenomenon. The high-[Mg^{2+}] relative mobility decreased in a fashion corresponding directly to the increasing mobility of the constrained nonfoldable P4-P6 relative to unconstrained nonfoldable P4-P6. Thus, the M_{high} parameter was corrected according to the data in Figure S3: $M_{obs} = (M_{low} + (M_{high}/c)\bullet K\bullet[Mg^{2+}]^n)/(1 + K\bullet[Mg^{2+}]^n)$, where the sole change is that (M_{high}/c) replaces M_{high} in the original titration equation. The value c is a empirical correction factor derived directly from the appropriate fit equation in the form of $c = a + b\bullet\log([Mg^{2+}])$.

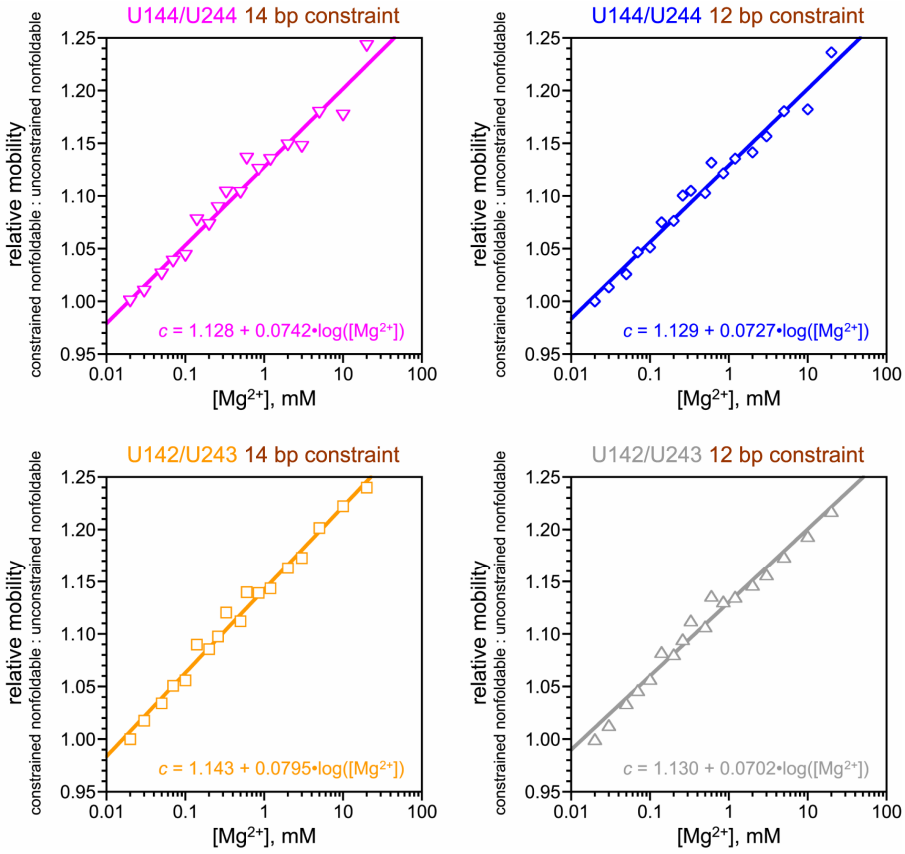

Figure S3. Relative mobility correction factors for the DNA-constrained RNAs. For each RNA, the mobility of the constrained nonfoldable variant relative to the unconstrained nonfoldable variant was determined. The relative mobility values were normalized by the same multiplicative factor such that the relative mobility was 1.00 at the lowest tested Mg^{2+} concentration of 0.02 mM, where relatively little compaction of the unduplexed DNA strands is expected. Each data set was fit to the empirical equation $c = a + b\bullet\log([Mg^{2+}])$.

In all cases, values of ΔΔG° were calculated as described,[3] with ΔG° for each RNA equal to $+n$RT•ln $[Mg^{2+}]_{1/2}$. ΔΔG° is defined as stated in the Figure 1 caption. Regardless of the fit value of n that was used along with K to compute $[Mg^{2+}]_{1/2}$, $n = 4$ was assumed in calculating all ΔΔG° values, as described[3] (the fit values of n were between 3.7 and 4.5). From the data in Figure 3B, the fit values of $[Mg^{2+}]_{1/2}$ were 0.24 ± 0.04, 0.29 ± 0.04, 0.31 ± 0.04, 0.46 ± 0.06, and 0.70 ± 0.04 mM. The corresponding computed values of ΔΔG° relative to unconstrained P4-P6 were –2.51 ± 0.39, –2.08 ± 0.35, –1.98 ± 0.34, and –1.00 ± 0.34 kcal/mol.

As an alternative fitting approach, the mobility of each DNA-constrained RNA can instead be calculated relative to the *unconstrained* nonfoldable P4-P6; i.e., P4-P6-bp *without* any attached DNA strands. Because in this analysis the reference RNA has no constraint strands at all, there should be no deviation from a flat baseline at high Mg^{2+} concentrations. Indeed, in titration plots analogous to those of Figure 3B, but now using the mobility computed relative to the unconstrained nonfoldable P4-P6, a flat baseline is observed at high Mg^{2+} concentrations (Figure S4). In addition, we now expect—and observe—

a modest deviation from a flat baseline at very *low* [Mg^{2+}], because at low [Mg^{2+}] the foldable RNA is in an unfolded state that has the DNA strands available for Mg^{2+}-induced compaction (Figure S2). Due to the DNA strand compaction, the foldable RNA begins to migrate relatively faster as the [Mg^{2+}] increases, but the reference RNA (which lacks DNA strands in this alternative fitting approach) maintains a constant mobility. Therefore, the relative mobility increases at very low [Mg^{2+}] (<0.1 mM) before P4-P6 itself begins to adopt substantial tertiary structure. The first fitting approach does not show this deviation from a flat baseline at very low [Mg^{2+}], because in that fitting approach both the foldable and reference RNAs have compactable DNA strands.

In the first fitting approach as used for Figure 3B, M_{high} was corrected by the empirical factor *c* derived from the data in Figure S3, which correlate the mobilities of the constrained and unconstrained nonfoldable P4-P6 RNAs. In the alternative fitting approach, we still must correct for the same physical phenomenon (i.e., Mg^{2+}-dependent compaction of DNA strands), but now M_{low} rather than M_{high} must be corrected. The revised fitting equation is $M_{obs} = ((M_{low} \bullet c) + M_{high} \bullet K \bullet [Mg^{2+}]^n)/(1 + K \bullet [Mg^{2+}]^n)$, where the sole change is now that ($M_{low} \bullet c$) replaces M_{low} in the original titration equation. The empirical correction factor *c* is exactly the same as determined in Figure S3 to enable the first fitting approach. Via the fits of Figure S4, the $[Mg^{2+}]_{1/2}$ values and corresponding ΔΔG° values are essentially unchanged from the first fitting approach (data not shown). This alternative fitting approach clearly illustrates that the deviation from a flat baseline can be induced to appear at either high or low [Mg^{2+}] depending on whether or not the reference RNA used for computing relative mobilities has attached DNA strands. Therefore, the deviation from a flat baseline is not inherent to either high or low [Mg^{2+}]. This is consistent with the empirical data in Figure S3, which show that compaction of the attached DNA strands occurs over the entire assayed Mg^{2+} concentration range when the P4-P6 is nonfoldable.

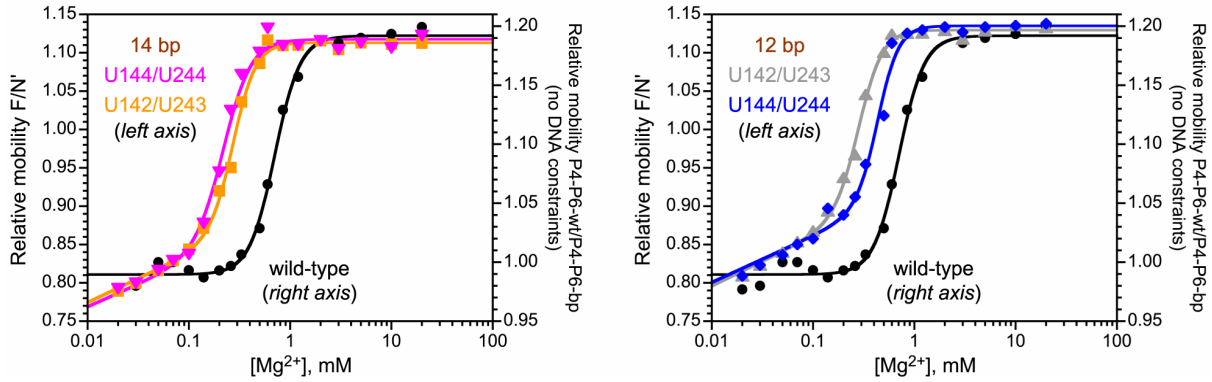

Figure S4. Data of Figure 3 replotted according to the alternative fitting approach (see text for full explanation). The mobility of each DNA-constrained P4-P6 variant (F) was computed relative to the unconstrained nonfoldable P4-P6; i.e., P4-P6-bp without attached DNA strands (N′; *left axis*). The mobility of wild-type P4-P6 without DNA strands was computed relative to P4-P6-bp also lacking attached DNA strands (*right axis*). P4-P6 lacking attached DNA strands inherently migrates faster than P4-P6 with attached DNA strands, due to the additional mass of the DNA. Therefore, the use of plots with two *y*-axes (i.e., double-*y* plots) allows the best visual comparisons among the data sets, while not altering the calculated $[Mg^{2+}]_{1/2}$ values.

References for Supporting Information

(1) Miduturu, C. V.; Silverman, S. K. DNA Constraints Allow Rational Control of Macromolecular Conformation. *J. Am. Chem. Soc.* **2005**, *127*, 10144-10145.
(2) Miduturu, C. V.; Silverman, S. K. Synthesis and Application of a 5′-Aldehyde Phosphoramidite for Covalent Attachment of DNA to Biomolecules. *J. Org. Chem.* **2006**, *71*, 5774-5777.
(3) Silverman, S. K.; Cech, T. R. Energetics and Cooperativity of Tertiary Hydrogen Bonds in RNA Structure. *Biochemistry* **1999**, *38*, 8691-8702.
(4) Murphy, F. L.; Cech, T. R. An Independently Folding Domain of RNA Tertiary Structure within the *Tetrahymena* Ribozyme. *Biochemistry* **1993**, *32*, 5291-5300.
(5) Miduturu, C. V.; Silverman, S. K. Modulation of DNA Constraints on Macromolecular Folding. *Angew. Chem. Int. Ed.* **2006**, *45*, 1918-1921.